A Structural Expression of *Exo*-Anomeric Effect

Elena R. Alonso, Isabel Peña, Carlos Cabezas, and José L. Alonso

Grupo de Espectroscopía Molecular (GEM), Edificio Quifima, Laboratorios de Espectroscopia y Bioespectroscopia, Unidad Asociada CSIC, Parque Científico UVa, Universidad de Valladolid, 47011 Valladolid, Spain

* E-mail: jlalonso@qf.uva.es.

ABSTRACT. Structural signatures for *exo*-anomeric effect have been extracted from archetypal methyl-β-D-xyloside using broadband Fourier transform microwave spectroscopy combined with laser ablation. Spectrum analysis allows determination of a set of rotational constants, which has been unequivocally attributed to conformer cc-β-$^4C_1$ g-, corresponding to the global minimum of the potential energy surface, where the aglycon residue (CH_3) orientation contributes towards maximization of the *exo*-anomeric effect. Further analysis allowed determination of r_s structure, based on the detection of eleven isotopologues – derived from the presence of six ^{13}C and five ^{18}O atoms - observed in their natural abundances. The observed glycosidic C_1-O_1 bond length decrease (1.38 Å) can be interpreted as derived from hyperconjugative interaction due to the *exo*-anomeric effect. As such, *exo*-anomeric effect presents itself as one of the main driving forces controlling the shape of many biologically important oligosaccharides.

**TOC GRAPHICS**
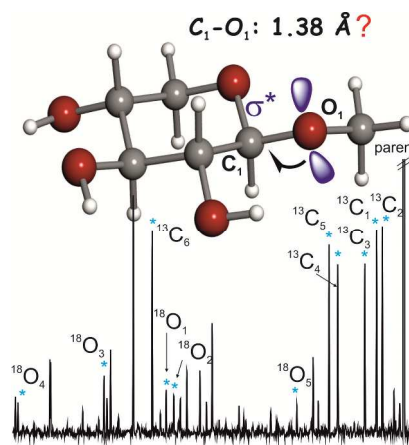
KEYWORDS. Microwave spectroscopy, laser ablation, conformational analysis, hydrogen bonding, glycoside.

TEXT. The anomeric effect refers to the propensity of polar substituents - bonded to an anomeric center - to occupy the axial (α-anomer) position rather than the equatorial (β-anomer) as would normally be expected in a monosaccharide chair conformation.[1-3] Such effect is thought to arise from either molecular orbital interactions or electrostatic interactions.[4-7] The most favored and accepted molecular orbital framework revolves around an interaction between an axially-located lone pair of electron in a molecular orbital (n) at the O_5 atom and an unoccupied anti-bonding molecular orbital (σ^*) of the C_1-O_1 bond (see axial acetals in Fig.1). Such antiperiplanar arrangement for the axial orientation favors this n→σ^* hyperconjugative interaction (back-bonding effect). Furthermore, if the axial exocyclic alkoxy -O-R group (aglycon) adopts the appropriate conformation, there is again an antiperiplanar arrangement of a molecular orbital (n) on O_1 and an unoccupied σ^* molecular orbital along the C_1-O_5 bond giving rise also to an extra anomeric effect[8] (see Fig. 1). Although no physical difference exists between both anomeric effects, two different terms, *endo*-and *exo*-anomeric, were introduced.[2,8] The standard *endo*-anomeric provides a driving force for the preference for the axial orientation of the aglycon in the six-membered glycopyranosides whereas the *exo*-anomeric effect influences the configuration adopted by the aglycon of the glycoside.
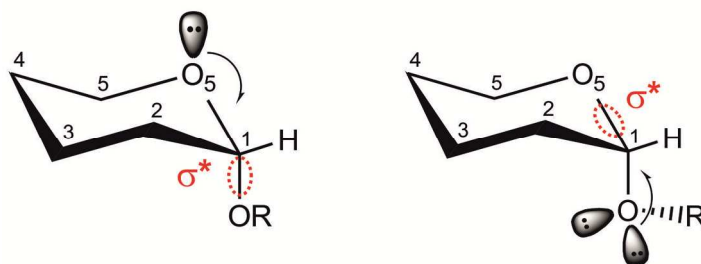
Figure 1. Axial acetals showing the *endo*-anomeric effect (left) which stabilizes the axial anomer and the antiperiplanar arrangement of the *exo*-cyclic alcoxy group for the *exo*-anomeric effect (right).
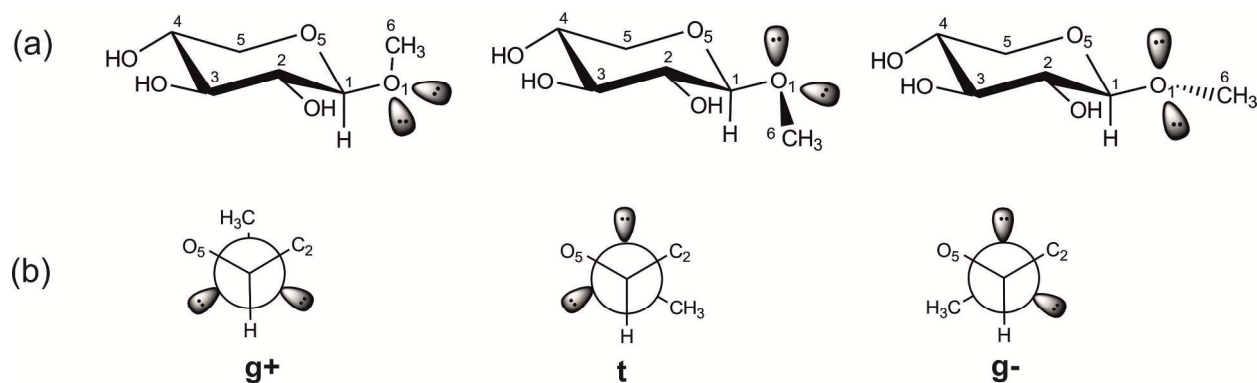
Figure 2. (a) The three plausible conformations of the aglycon in methyl β-D-xyloside with a $^4C_1$ chair configuration (C_4 carbon is above the reference plane $C_2C_3C_5O_5$ and C_1 carbon is found below it); the lone pair electrons on O_1 are shown as in sp^3 orbitals. (b) Newman projections along C_1–O_1 bond; the symbols g+ (+60º), t (180º) and g- (-60º) have been used to denote the values of the torsion angle $\varphi = C_6$-O_1-C_1-O_5.

Oppositely, in an equatorial acetal (see Fig. 2) - where no contribution from the *endo*-anomeric effect exists -, it is the *exo*-anomeric effect that prevails and thus dictates the preferred conformation of the alkoxy group at the anomeric C_1 carbon atom, seemingly being responsible for the conformational preferences around glycopyranoside linkages as well as the helical shape of various polysaccharide chains. Thus, any considerations on the conformational properties of glycopyranosides would require the determination of the torsional angle $\varphi = C_6$-O_1-C_1-O_5 defined by the aglyconic carbon and the oxygen atom of pyranose ring (Fig. 2b). This is of paramount importance for shape determination of many biologically important oligosaccharides.[9]

A large volume of experimental results on glycosides, dating back to those obtained in condensed phases by NMR[10] and X-ray investigations,[11,12] already pointed towards the existence of *endo*- and *exo*-anomeric effects in the observed conformational preferences. Conversely, the existence of an *exo*-anomeric effect was later brought into question in the literature through a series of studies on C-glycosides – where the glycosidic oxygen atom had been replaced by a methylene group[13,14] and were found to exhibit the same preferred conformations as their O-glycosides analogues, despite the inexistence of the lone pair effects.

It is generally accepted that all above-mentioned results in condensed phases are strongly influenced by environmental effects[15] associated with the solvent or crystal lattice interactions that may subtly mask the anomeric effect. As such, investigations have been recently conducted in gas phase isolation conditions, in order to overcome such shortcomings. The presence of the anomeric effect has been probed *via* ''ion-dip'' vibrational spectroscopy (IRID) of the doubly and triply hydrated α and β anomers of phenyl D-mannopyranoside isolated under molecular beam conditions.[16] Subtle differences in the vibrational signatures of both hydrated α and β anomers were interpreted by complementary theoretical calculations and ascribed to the anomeric effect. In the same context, complexes formed between the N-Acetyl-L-phenylalanine methylamide and the α or β-anomers of D-galactose isolated in the gas phase were used to sense the *exo*- and *endo*-anomeric effect using a combination of laser spectroscopy and computational analysis.[17] Surprisingly, these results were recently brought into question by Wang et al.,[18] who provided strong computational evidence showing that the observed spectral changes attributed to the anomeric effect simply come from the conformational differences between the α- and β-anomers.

The above scenario highlights the importance of a benchmark investigation on glycoside to determine its intrinsic conformational and structural properties, thus avoiding intricate and rather speculative spectroscopic interpretations. In the present work, we report the first experimental investigation of the archetypal acetal methyl-β-D-xyloside ($C_6H_{12}O_5$, Fig.2) isolated in gas phase, probing for convincing structural evidences of the *exo*-anomeric effect. The major problem of working with gas-phase carbohydrates due to their solid samples labile nature and inherent vaporization difficulties has been overcome. Indeed, in latest years, a number of powerful strategies have been established in our lab, involving the use of laser ablation for
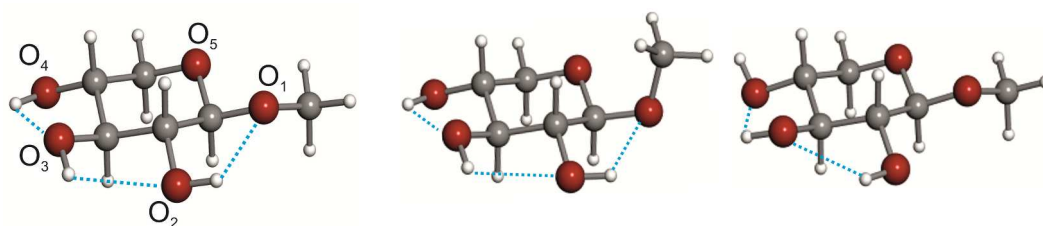
vaporizing intact molecules of solid samples of a biomolecule into gas phase, followed swiftly

by a rapid cooling in a free jet expansion, thus stabilize their conformational panorama, and

highly selective Fourier-transform microwave spectroscopy to allow probing of such structures.[19]

Such methodology constitutes a powerful tool in gas phase studies of isolated sugars, as it has

been recently shown for the representative D-glucose[20] and many other monosaccharides.[21-25]

The combination of broadband chirped pulse Fourier-transform microwave techniques[26] (CP-

FTMW), and picosecond laser ablation (LA),[27] has allowed the conformational study of methyl

β-D-xyloside. The broadband rotational spectrum of laser ablated methyl β-D-xyloside

comprehended within the 6-12 GHz region is shown in Figure 3. Apart from known

photofragmentation lines common to other carbohydrates, the spectrum is dominated by intense

μ_a-type R-branch progressions belonging to a rotamer exhibiting a characteristic pattern of a

nearly prolate asymmetric rotor. Much weaker μ_b- and μ_c-type transitions were also assigned and

measured. A total of 64 transitions (Table S1 in the Supporting Information) were included in a

rigid rotor analysis[28] to give the set of experimental rotational constants collected in first column

of Table 1.
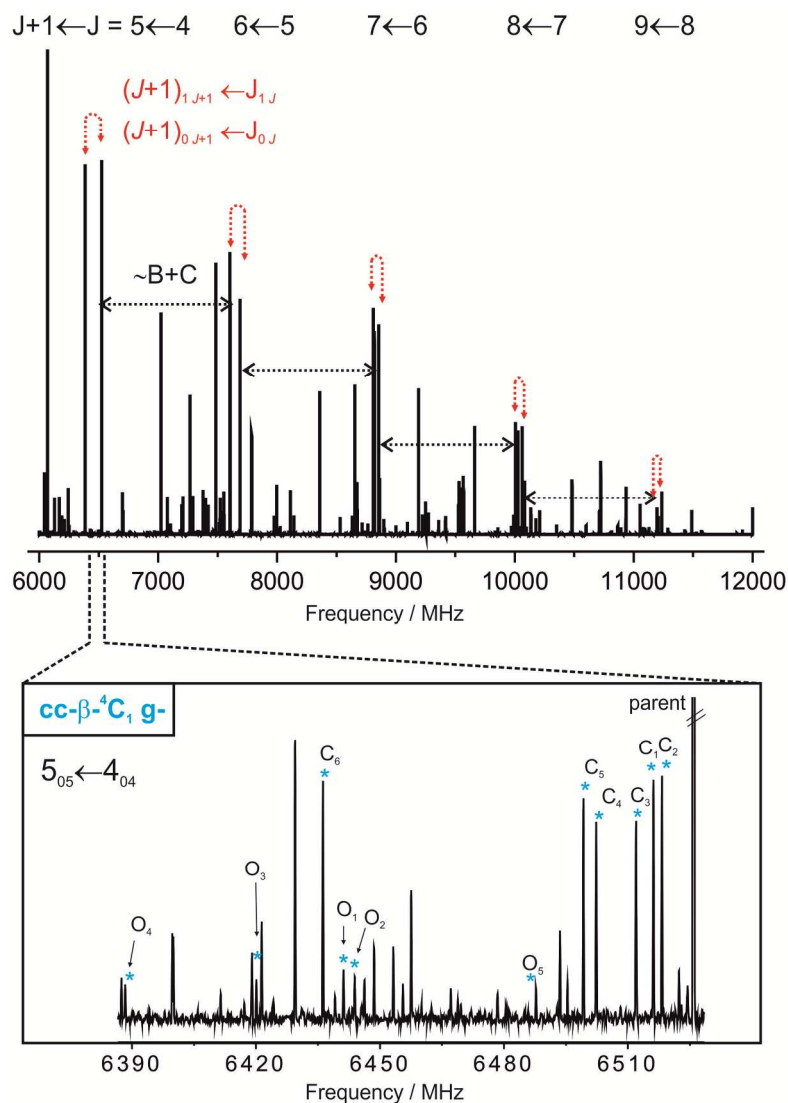
Figure 3. Broadband spectrum of methyl β-D-xyloside from 6 to 12 GHz (110000 fids) showing the intense sets of μ_a-type R-branch transitions separated approximately B + C with J ranging from 4 to 8, belonging to the observed rotamer. a-type $(J+1)_{1\ J+1}\leftarrow J_{1\ J}$ and $(J+1)_{0\ J+1}\leftarrow J_{0\ J}$ pairs of rotational progressions (becoming degenerated with increasing J) are indicated. The photofragmentation products have been discarded in the analysis. Inset: the $5_{05}\leftarrow4_{04}$ rotational transition for the six ^{13}C and five ^{18}O isotopologues of the observed cc-β-^{4}C$_1$ g- conformer.

Table 1. Experimental rotational parameters for the observed rotamer of methyl β-D-xyloside in comparison with those predicted *ab initio*[a] for the most stable conformers (within 1400 cm^{-1}).

	Experimental	cc-β-^{4}C$_1$ g- [g]	cc-β-^{4}C$_1$ g+	c-β-^{4}C$_1$ g-
A[b]	1766.25692 (72)[e]	1771.6	1713.1	1774.5
B	829.25439 (24)	833.0	868.7	829.1
C	592.91443 (17)	595.4	638.0	595.3
$\|\mu_a\|$	Intense [f]	2.1	1.4	2.0
$\|\mu_b\|$	Weak	0.5	0.9	2.9
$\|\mu_c\|$	Weak	0.8	0.9	0.5
ΔE[c]	-	0	1106	1448
ΔG[d]	-	0	1069	1230

[a] MP2/6-311++G(d,p) level of theory. [b] A, B, and C represent the rotational constants (in MHz); $\|\mu_a\|$, $\|\mu_b\|$ and $\|\mu_c\|$ are the absolute values of electric dipole moment components (in D). [c] Relative electronic energies (in cm^{-1}). [d] Gibbs energies calculated at 298 K (in cm^{-1}). [e] Standard error in parentheses in the units of the last digit. [f] Qualitative intensity of the type of spectrum observed. [g] The notation used to label the different conformers include the symbols "*c*" or "*cc*" to indicate a clockwise or counterclockwise configuration of the adjacent OH bonds, respectively, "β" to label the anomer type, "^{4}C$_1$" to denote the pyranose chair form and "g+" or "g-" to label the torsion angle φ = C$_6$-O$_1$-C$_1$-O$_5$.

In the identification of the observed rotamer as a particular conformer of methyl β-D-xyloside, structures exhibiting the most stable ^{4}C$_1$ chair configuration, with all substituents in the equatorial orientation, were considered first. *Ab initio* calculations,[29] were carried out on the three plausible configurations of the aglycon defined through the torsion angle φ (see Fig.2). The theoretical requirement for a maximum *exo*-anomeric effect corresponds to that where the aglycon is oriented in such a way that the O$_1$ *sp^3* (n) orbital is in an anti-periplanar orientation with regard to the O$_5$-C$_1$ bond, thus maximizing the overlap with the σ* orbital. Two such orientations are possible, displayed in the **g+** (φ ~ 60º) and **g-** (φ ~ -60º) configurations. Configuration **t** (Ø~ 180º) is *a priori* disfavored by ordinary steric interactions and it is not

comprised in the three pyranose forms **cc-β-^{4}C$_1$ g-**, **cc-β-^{4}C$_1$ g+** and **c-β-^{4}C$_1$ g-** shown in Table 1 predicted in an energy window of 1400 cm^{-1}. A first comparison between experimental and theoretical rotational constants values collected in Table 1 clearly indicates that the experimental rotational constants values are consistent with those predicted for conformers **cc-β-^{4}C$_1$ g-** and **c-β-^{4}C$_1$ g-**. Both conformers present the same aglycon "g-" configuration stabilized by the *exo*-anomeric effect but differ in the intramolecular H-bond networks that takes place for each configuration, which are strongly reinforced by σ-hydrogen-bond cooperativity.[30] Thus, the conformational analysis of methyl β-D-xyloside requires the consideration of the subtle variation in hydroxyl arrangement which are relevant to distinguish between different conformations. Hence, the most stable form **cc-β-^{4}C$_1$ g-** presents a counter-clockwise (*cc*) arrangement of three intramolecular hydrogen bonds O$_4$H···O$_3$H···O$_2$H··O$_1$CH$_3$, while the less stable **c-β-^{4}C$_1$ g-** shows a chain of two cooperative hydrogen bonds O$_2$H···O$_3$H···O$_4$H orientated clockwise (*c*). This does not, however, significantly affect their rotational constants values and, as such, discrimination based solely on the values of the experimental rotational constants values is not possible. Yet, the *cc* and *c* arrangements do drastically alter μ$_b$ dipole moment component value, changing from 0.5 D to 2.9 D when passing from the **cc-β-^{4}C$_1$ g-** conformer to **c-β-^{4}C$_1$ g-** and, consequently, affect the intensity of observable type of transitions. Table 1 documents that the observed rotamer shows intense μ$_a$-type transitions and weak μ$_b$- and μ$_c$-type transitions. Therefore, conformer **c-β-^{4}C$_1$ g-** should be excluded due to the large predicted value for the b dipole moment component. Thus, the observed rotamer can only be ascribed as **cc-β-^{4}C$_1$ g-** conformer. This is in good agreement with the predicted *ab initio* relative energies, which point out conformer **cc-β-^{4}C$_1$ g-** as the global minimum.

Table 2. Experimental rotational parameters for the observed ^{13}C isotopologues of methyl β-D-xyloside.

Parameter	C_1	C_2	C_3	C_4	C_5	C_6
A^a /MHz	1765.9994 (66)[b]	1760.1576 (87)	1763.7850 (65)	1762.1361 (53)	1747.032 (10)	1763.9109 (55)
B /MHz	827.44527 (35)	829.16223 (25)	827.18114 (25)	825.74089 (22)	828.88609 (48)	813.35867 (27)
C /MHz	592.01546 (30)	592.26157 (32)	591.64010 (20)	590.75622 (18)	590.58159 (38)	584.53354 (22)
σ^c / kHz	6.8	6.2	4.0	3.7	7.6	5.7
N^d	23	18	16	18	19	25

[a]A, B and C are the rotational constants. [b]Standard error in parentheses in units of the last digit. [c]rms deviation of the fit. [d]Number of measured transitions.

Table 3. Experimental rotational parameters for the observed ^{18}O isotopologues of methyl β-D-xyloside.

Parameter	O_1	O_2	O_3	O_4	O_5
A^a /MHz	1764.640 (16)[b]	1706.411 (35)	1738.630 (14)	1748.195 (18)	1742.544 (14)
B /MHz	813.81270 (70)	828.31433 (98)	816.0187 (22)	808.02371 (66)	827.4055 (10)
C /MHz	585.02862 (51)	585.79520 (97)	583.2463 (10)	580.19362 (57)	589.59210 (43)
σ^c / kHz	5.6	8.9	5.7	7.6	6.2
N^d	8	10	7	9	9

[a]A, B and C are the rotational constants. [b]Standard error in parentheses in units of the last digit. [c]rms deviation of the fit. [d]Number of measured transitions.

Table 4. Substitution (r_s) structure for conformer cc-β-^{4}C$_1$ g- of methyl β-D-xyloside and comparison with *ab initio* calculations. Distances in Å and angles in degrees.

Bond distances	Gas phase[a]	*Ab initio*[b]	Angles	Gas phase[a]	*Ab initio*[b]
C_5–O_5	1.4047 (52)[c]	1.426	C_1–O_5–C_5	110.93 (34)[c]	110.71
O_5–C_1	1.477 (31)	1.416	C_1–C_2–C_3	111.06 (78)	109.29
C_1–C_2	1.526 (26)	1.522	C_2–C_3–C_4	110.45 (34)	110.06
C_2–C_3	1.435 (17)	1.515	C_3–C_4–C_5	108.64(29)	109.17
C_3–C_4	1.5072 (43)	1.517	C_6–O_1–C_1	116.0 (12)	112.72
C_4–C_5	1.5434(43)	1.524	O_1–C_1–O_5	106.1 (14)	109.50
C_1–O_1	**1.3816 (77)**	**1.387**	C_5–O_5–C_1–C_2	-61.90 (92)	-63.57
O_1–C_6	1.4209 (54)	1.427	O_5–C_1–C_2–C_3	59.33 (65)	58.62
C_2–O_2	1.4435 (63)	1.421	C_1–C_2–C_3–C_4	-58.0 (10)	-54.17
C_3–O_3	1.4327 (39)	1.422	C_2–C_3–C_4–C_5	55.82 (73)	53.89
C_4–O_4	1.4190(34)	1.418	C_3–C_4–C_5–O_5	-57.99 (71)	-57.94
			C_4–C_5–O_5–C_1	62.45 (94)	63.36
			O_1–C_1–O_5–C_5	176.78 (78)	178.64
			C_6–O_1–C_1–O_5	**-68.45 (75)**	**-67.76**
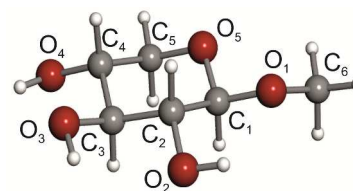
[a] This work. [b]MP2/6-311++G(d,p) level of calculation. [c] Derived errors in parentheses in units of the last digit following reference 32.

A closer inspection into the low intensity background of the spectrum did not reveal the existence of spectral signatures attributable to the **cc-β-^{4}C$_1$ g+.** However, on the low frequency side of each intense μ$_a$-type R-branch transition of the observed **cc-β-^{4}C$_1$ g-** conformer, very

weak sets of the same R-branch progressions could be identified and were indeed ascribed to six

monosubstituted ^{13}C and five [18]O species of the parent molecule observed in their natural

abundance of 1.1% and 0.2%, respectively. Isotopic progressions for the $5_{05} \leftarrow 4_{04}$ rotational

transition are shown in the inset of Fig. 3. Predicted frequency shifts for the **cc-β-$^4C_1$ g-**

conformer were found to be consistent with those observed experimentally, further supporting

the identification of this conformer in the supersonic expansion. More than 150 rotational

transitions were measured (Tables S5-S15) for the eleven isotopic species and used in a rigid

rotor analysis[28] to give the experimental rotational constants collected in Tables 2 and 3. The

isotopic information was then used to derive the substitution structure[31,32] shown in Table 4

(atomic coordinates in Table S16 in the Supporting Information).

The *exo*-anomeric effect and hydrogen bonding are the main factors controlling the

conformational behavior of the archetypal methyl β-D-xyloside, represented by conformer **cc-β-**

$^4C_1$ g-, where hydroxyl groups are preferentially orientated in such way as to yield cooperative

hydrogen bonding as efficiently as possible. The highly detailed picture obtained for this

conformer provides new insights into the *exo*-anomeric effect, which is particularly expressed in

the determined glycosidic structure. Hence, the determined value for the torsion angle φ (= C_6-

O_1-C_1-O_5) of -68º in the observed conformer is consistent with a "g-" conformation of the

aglycon that maximize the *exo*-anomeric effect. Thus, the importance of the *exo*-anomeric effect

is unchallenged, and it may be seen as the main driving force influencing the aglycon structure,

dominating over all other factors that are likely to. Nonetheless, the most important feature of the

structural data presented in Table 4 is the fact that the determined value for the glycosidic C_1-O_1

bond (1.38 Å) is shown to be substantially shorter than the normal C-O bonds, typically ranging

between 1.42-1.44 Å.[33,34] Although there are conflicting theoretical reports[35] regarding the origin

of the anomeric effect, the observed shortening of the C_1-O_1 bond can be interpreted in light of the currently popular hyperconjugative explanation for the *exo*-anomeric effect. The *ab initio* structure, also collected in Table 4, is in excellent accordance with our experimental results, which provide an invaluable benchmark to validate *ab initio* computations.

Given the great sensitivity reached with our LA-CP-FTMW technique and the relevance of glycosidic linkages in biology, further investigation on other biologically relevant glycosides have been undertaken to improve our understanding of the key roles that anomeric and *exo*-anomeric effects play in current organic chemistry.

EXPERIMENTAL SECTION

A sample of methyl β-D-xyloside (m.p. 155−158 °C) was used without further purification, and prepared by mixing the compound powder with a commercial binder. The mixture was pressed to form cylindrical rods, which were placed in a laser ablation nozzle[27] to be vaporized using a 20 ps Nd:YAG laser (12 mJ/pulse). The vaporized sample was then seeded in the Ne carrier gas at backing pressure of 18 bar, to expand adiabatically into the vacuum chamber, and probed by broadband CP-FTMW spectroscopy.[27] Up to 110 000 individual free induction decays at a 2 Hz repetition rate were averaged in the time domain and Fourier transformed to obtain the broadband frequency domain spectrum from 6 to 12 GHz.

ASSOCIATED CONTENT

Supporting Information. Complete list of transition frequencies measured for the most abundant conformer of methyl β-D-xyloside and their isotopologues. Cartesian coordinates for the most stable conformers and substitution coordinates for conformer cc-β-$^4C_1$g-. Complete reference 29. This material is available free of charge via the Internet at http://pubs.acs.org.

AUTHOR INFORMATION

Corresponding Author

*Email: jlalonso@qf.uva.es

REFERENCES

(1) Edward, J.T. Stability of glycosides to acid hydrolysis. *Chem. Ind. (Lond.)* **1955**, 36, 1102-1104.

(2) Lemieux, R. U.; Chü, P. in *133rd National Meeting of the American Chemical Society* 31N (American Chemical Society, 1958).

(3) Lemieux, R.U. Molecular Rearragements. John Wiley and Sons, New York, 1964, p.709 and references therein.

(4) Juaristi, E.; Cuevas, G. Recent Studies of the Anomeric Effect. *Tetrahedron* **1992**, *48*, 5019-5087 and references therein.

(5) Perrin, C. L.; Armstrong, K. B.; Fabian, M. A. The origin of the anomeric effect: conformational analysis of 2-methoxy-1,3-dimethylhexahydropyrimidine. *J. Am. Chem. Soc.* **1994**, *116*, 715-722 and references therein.

(6) Juaristi, E.; Cuevas, G. The Anomeric Effect. CRC Press, 1995 and references therein.

(7) Tvaroska, I. & Bleha, T. Anomeric and exoanomeric effects in carbohydrate chemistry. *Adv. Carbohydr. Chem. Biochem.* **1989**, *47*, 45-123.

(8) Lemieux, R. U.; Koto, S.; Voisin, D. The Exo-Anomeric Effect. *ACS Symposium Series*, **1979**, *87*, Chapter 2, 17-29.

(9) Meyer, B. Conformational Aspects of Oligosaccharides. *Topics Curr. Chem.* **1990**, *154*, 141-208.

(10) Lemieux, R.U.; Koto, S. Conformational properties of glycosidic linkages. *Tetrahedron* **1974**, *30*, 1933-44.

(11) Berman, H. M.; Chu, S.S.C.; Jeffrey, G. A. Anomeric Bond-Character in the Pyranose Sugars. *Science* **1967**, *157*, 1576-1577.

(12) Brown, C. J.; Cox, G.; Llewellyn, F. J. The Crystalline Structure of the Sugars. Part V. A Three-dimensional Analysis of Methyl β-Xyloside. *J. Chem. Soc. (A)* **1966**, 922-927.

(13) Goekjian, P. G.; Wu, T.-C.; Kishi, Y. Preferred Conformation of C-Glycosides. 6. Conformational Similarity of Glycosides and Corresponding C-Glycosides. *J. Org. Chem.* **1991**, *56*, 6412-6422.

(14) Goekjian, P. G.; Wu, T.-C.; Kang, H.-Y.; Kishi, Y. Preferred Conformation of C-Glycosides. 7. Preferred Conformation of Carbon Analogues of Isomaltose and Gentiobiose. *J. Org. Chem.* **1991**, *56*, 6422-6434.

(15) Lemieux, R.U. Newer developments in the conformational analysis of carbohydrates. Pure Appl. Chem. **1971**, *27*, 527-548.

(16) Mayorkas, N.; Rudic, S.; Davis, B.G.; Simons, J. P. Heavy water hydration of mannose: the anomeric effect in solvation, laid bare. *Chem.Sci.* **2011**, *2*, 1128-1134.

(17) Cocinero, E. J.; Çarçabal, P.; Vaden, T. D.; Simons, J. P.; Davis, B. G. Sensing the anomeric effect in a solvent-free environment. *Nature* **2011**, *469*, 76-79.

(18) Wang, C.; Ying, F.; Wu, W.; Mo, Y. Sensing or No Sensing: Can the Anomeric Effect Be Probed by a Sensing Molecule?. *J. Am. Chem. Soc.* **2011**, *133*, 13731–13736.

(19) Alonso, J. L.; López, J. C. "Microwave Spectroscopy of Biomolecular Building Blocks" *Top. Curr. Chem.* **2015**, *364*, 335-402, Springer International Publishing Switzerland.

(20) Alonso, J. L.; Lozoya, M. A.; Peña, I.; López, J. C.; Cabezas, C.; Mata, S.; Blanco, S. The conformational behaviour of free D-glucose-at last. *Chem. Sci.* **2014**, *5*, 515-522.

(21) Peña, I.; Cabezas, C.; Alonso, J. L. Unveiling epimerization effects: a rotational study of α-D-galactose. *Chem. Commun.* **2015**, *51*, 10115-10118.

(22) Peña, I.; Mata, S.; Martín, A.; Cabezas, C.; Daly, A. M.; Alonso, J. L. Conformations of D-xylose: the pivotal role of the intramolecular hydrogen-bonding. *Phys. Chem. Chem. Phys.* **2013**, *15*, 18243-18248.

(23) Bermúdez, C.; Peña, I.; Cabezas, C.; Daly, A. M.; Alonso, J. L. Unveiling the Sweet Conformations of D-Fructopyranose. *ChemPhysChem* **2013**, *14*, 893-895.

(24) Peña, I.; Cocinero, E. J.; Cabezas, C.; Lesarri, A.; Mata, S.; Écija, P.; Daly, A.M.; Cimas, A.; Bermúdez, C.; Basterretxea, F. J.; Blanco, S.; Fernández, J. A.; López, J. C.; Castaño, F.; Alonso, J. L. *Angew. Chem., Int. Ed.* **2013**, 52, 11840-11845.

(25) Cabezas, C.; Peña, I.; Daly, A. M.; Alonso, J. L. Erythrose revealed as furanose forms. *Chem. Commun.* **2013**, *49*, 10826-10828.

(26) Brown, G. G.; Dian, B. C.; Douglass, K. O.; Geyer, S. M.; Shipman, S. T.; Pate, B. H. A broadband Fourier transform microwave spectrometer based on chirped pulse excitation. *Rev. Sci. Instrum.* **2008**, *79*, 053103.

(27) Mata, S.; Peña, I.; Cabezas, C.; López, J. C.; Alonso, J. L. A broadband Fourier-transform microwave spectrometer with laser ablation source: The rotational spectrum of nicotinic acid *J. Mol. Spectrosc.* **2012**, *280*, 91-96.

(28) Gordy, W.; Cook, R. L. *Microwave Molecular Spectroscopy*, John Wiley & Sons, New York, **1984**.

(29) Frisch, M. J.; et al., Gaussian, Inc., Wallingford, CT, 2009; Calculations carried out at our 'Olimpo' Beowulf Cluster facility, recently installed in our laboratory.

(30) Jeffrey, G. A.; Saenger, W. Hydrogen Bonding in Biological Structures, Springer, New York, 1991.

(31) Kraitchman, J. Determination of Molecular Structure from Microwave Spectroscopic Data. *Am. J. Phys.* **1953**, *21*, 17-24.

(32) Van Eijck, B. P. Influence of molecular vibrations on substitution coordinates. *J. Mol. Spectrosc.* **1982**, *91*, 348-362.

(33) K. Kuchitsu, "Structure of Free Poliatomic Molecules", Springer-Verlag Berlin Heidelberg New York, 1998.

(34) Anslyn, E.V.; Dougherty, D. A. "Modern Physical Organic Chemistry" University Science Book, Sausalito, 2006.

(35) Mo, Y. Computational evidence that hyperconjugative interactions are not responsible for the anomeric effect. *Nature Chemistry* **2010**, *2*, 666-671.